

Liquid-Like Phases Preorder Peptides for Supramolecular Assembly

Rolando F. Rengifo⁺, Anthony Sementilli⁺, Youngsun Kim, Chen Liang, Noel Xiang'An Li, Anil K. Mehta,* and David G. Lynn*^[a]

Controlling supramolecular assembly remains a major challenge for materials science and synthetic biology. Biopolymers organize into multimolecular architectures via two-step nucleation processes involving dynamic intermediate solute-rich phases. Here we present spectroscopic analyses of metastable phases formed with a congener of the Alzheimer's disease A β peptide that reveals diverse populations of single β -sheets. The degree of order in this liquid-like particle phase is remarkable both in the range of sheets and the selection of a single propagating nucleus. The resulting fibril seed is less stable in solution and cooperatively transforms into another fibril. The conformational dynamics of this peptide provide a mechanistic model for controlling the range of polymorphic amyloid assemblies in health and disease.

From simple salts^[1] to complex biopolymers,^[2] self-assembly in aqueous environments proceeds through nucleation-dependent phase transitions following Ostwald's step rule.^[3] Protein misfolding diseases also transition through these dynamic solute-rich phases.^[1-2,4] In disease, polymorphism is prevalent in the assembled amyloid structures,^[5] suggesting that multiple nuclei may appear within the disordered phase. Such diversity may underlie the ability of external templates^[6] as diverse as nucleic acids^[7] to rapidly nucleate the propagation of distinct assemblies from these peptide-rich liquid phases.^[6a,8] To explore how these intermediate liquid-like phases might pre-order peptide nucleation, we sought metastable particle phases accessible to detailed spectroscopic structural analyses.

The oligomer cascade hypothesis^[8b,9] of Alzheimer's disease holds that the $A\beta$ peptide transitions via an initial liquid-like particle phase in the propagation of disease. Two simple $A\beta$ congeners, KLVFFAE^[8b] and KLVFFAQ,^[10] also undergo multistep nucleation via a metastable phase. Extensive fluorescence analyses in solution^[8f,g] and electron microscopy of dried samples^[8b] have provided evidence for a liquid-solid transition

occurring within the intermediate solute-rich particles en route to anti-parallel out-of-register β -sheets. $^{[6b,10]}$ These metastable particles have been challenged with preassembled peptides of distinct parallel or antiparallel β -sheets arrangements and these seeds successfully nucleate supramolecular propagation. Unfortunately, these intermediate particles proved to be too unstable under these conditions for detailed structural analyses.

Lengthening the peptide slightly and removing the C-terminal residue gave His-His-Gln-Ala-Leu-Val-Phe-Phe-Ala-NH $_2$ (K16A), as a more robust congener of A β . In 25 mM MES buffer at pH 5.6 and 25 °C, this peptide transitions through intermediate oligomeric particles with widths spanning 28 to 35 nm (Figure 1A, Figure S1) en route to fibers containing parallel in-register β -sheets. Bb., 11d, 12 When immature assemblies are centrifuged at 6792×g for 90 min in 4 °C, the pellet is enriched in long fibers with persistence lengths > 1 μm and diameters of 3.49 \pm 0.25 nm (Figure 1B, S2). The intermediate spherical oligomers retained in the supernatant are stable and

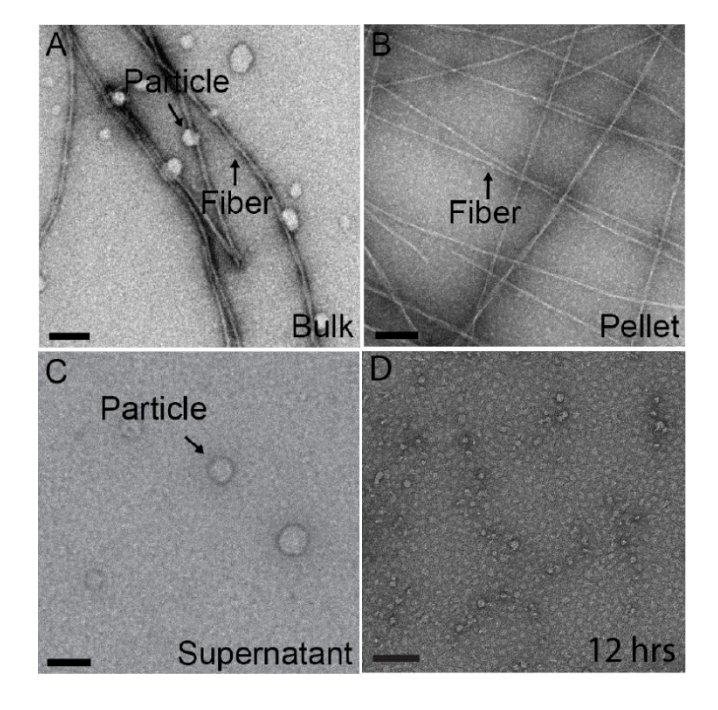


Figure 1. (A) TEM micrographs of HHQALVFFA-NH₂ peptides, after 10 days of assembly at 25 °C in 25 mM MES at pH 5.6, show predominantly fibers and particles. TEM of the pellet (B) and supernatant (C) after centrifugation at $6792 \times g$ for 90 min at 4 °C. For comparison, (D) TEM at 12 h of assembly. Scale bar = 100 nm.

[[]a] Dr. R. F. Rengifo,* A. Sementilli,* Y. Kim, Dr. C. Liang, Dr. N. X.'A. Li, Dr. A. K. Mehta, Dr. D. G. Lynn Chemistry Department Emory University 1515 Dickey Drive, Atlanta, GA 30322 E-mail: anil.mehta@ufl.edu dlynn2@emory.edu

^[+] These authors contributed equally to this work.

Supporting information for this article is available on the WWW under https://doi.org/10.1002/syst.202000007

readily visualized when dried on TEM grids, and are larger than the particles observed initially in the assembly (Figure 1C–D).

Previous attempts to detect early nucleation events have used metals to enhance TEM contrast within the intermediate particles [8b,11d,13], but metals can also template amyloid assembly. In this peptide, metals introduce conformational heterogeneity (Figure S3), probably due to diverse metal/histidine associations, and resolution of fibrous nuclei is not possible. In contrast, circular dichroism (CD) analyses during assembly provides clear evidence for a cooperative transition to β -sheets at 3.8 \pm 0.17 days (Figure 2A), a transition time consistent with the appearance of fibers by TEM (Figure S4).

Attenuated total reflectance isotope-edited (IE) FTIR spectra have greatly extended assignments in the assembly of similar peptides. [6,8d,e,14] While the early vibrational spectra recorded during the assembly of H-HHQALVF[1-13C]FA-NH2 contain low signal-to-noise (Figure 2B, S6), this system exhibits extended βsheet H-bonding signatures almost immediately. The absorptions at $1640~\text{cm}^{-1}$ and $1608~\text{cm}^{-1}$ (Figure S6) are most consistent with anti-parallel β -sheet assemblies, but these modes cooperatively transition as the fibers appear in solution. [6b,10] The final red-shifted ¹²C and ¹³C amide-I stretches at 1629 cm⁻¹ and 1606 cm⁻¹ and the corresponding drop in the ¹³C band intensity are consistent with a cooperative transition from anti-parallel to parallel β -sheets. [6b,10,14] This orientation transition, occurring at 4.7 ± 0.67 and 4.3 ± 0.44 days for band splitting and the height ratio of the amide-I band respectively, correlates with the transition time observed by CD.

To validate this early anti-parallel orientation in the initial particle phase, a $^{13}\text{C}/^{15}\text{N}$ enrichment scheme was designed to quantify specific $^{13}\text{C}-^{13}\text{C}$ and $^{13}\text{C}-^{15}\text{N}$ distances by NMR (Figure 3). The expected intramolecular distance between the ^{13}C carbonyl of Ala4 and the ^{15}N of Phe7 in an extended strand is predicted to be ~ 7 Å, but with peptides organized in parallel β -sheets, the intermolecular $^{13}\text{C}-^{13}\text{C}$ distance between H-bonded strands (Figure 3E) should be detectable with ^{13}C DQF-DRAWS solid-state NMR experiments. With anti-parallel β -sheets, the Ala carbonyl $^{13}\text{C}'s$ are too far apart in adjacent peptides for detection, but distances to the $^{15}\text{N}'s$ on adjacent strands (Figure 3F) should be accessible with $^{13}\text{C}\{^{15}\text{N}\}\text{REDOR}$ experiments.

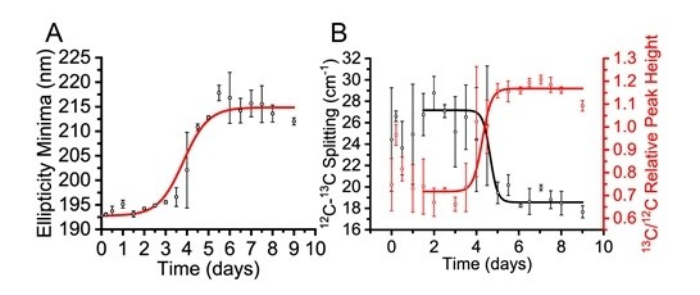


Figure 2. (A) Time-dependent CD showing a red shift of λ_{min} ellipticity of a 1 mM HHQALVFFA-NH $_2$ peptide solution at 25 °C. (B) FT-IR 12 C- 13 C splitting (black) and 13 C/ 12 C intensity ratio (red) for enriched (HHQ[1- 13 C]ALV[15 N]FFA-NH $_2$) under identical conditions. The 12 C amide-I band is at 1640 cm $^{-1}$ at t=0 and 1629 cm $^{-1}$ in fibers.

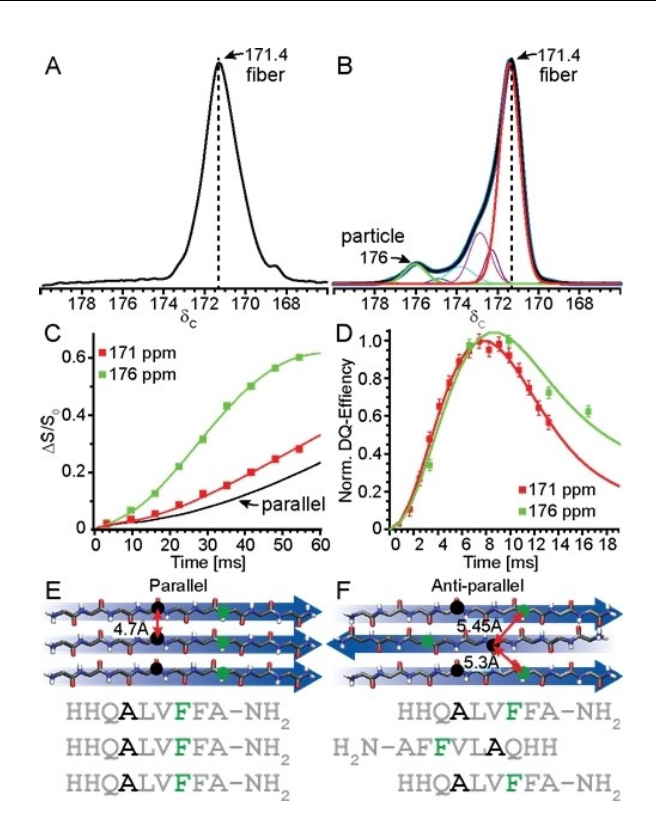


Figure 3. NMR analyses of isotope-enriched HHQ[1- 13 C]ALV[15 N]FFA-NH₂ assembled in pH 5.6 25 mM MES buffer at 25 °C. (A) 13 C CP-MAS NMR spectrum of lyophilized fibers and (B) in a mixture containing particles and fibers with individual contributing components indicated with colored lines. (C) 13 C{ 15 N}REDOR dephasing for resonances at 171.4 ppm (red squares) and 176 ppm (green squares). The 171.4 ppm resonance fits (red line) to a mixture of 92.9 \pm 1.4% parallel and 7.1 \pm 3.2% anti-parallel β-sheets. The predicted dephasing for fibers assembled with 100% parallel β-strands is represented by the solid black line. The 176 ppm resonance fits (green line) to 65% anti-parallel β-strands. (D) Normalized DQF-DRAWS experimental data for fibers with chemical shift at 171 ppm (red squares) and particles (green squares) fit to an array of 13 C's separated by 4.7 Å in parallel β-strands (solid lines). Models of (E) parallel and (F) anti-parallel β-sheets. [$^{1-13}$ C]Ala indicated with black circles/letters and [15 N]Phe with green circles/letters.

Isotopically enriched HHQ[1-¹³C]ALV[¹⁵N]FFA-NH₂ was prepared by solid-phase synthesis and allowed to assemble for 6 days before being concentrated via centrifugation at 4°C (Figure 1B). The supernatant was decanted and the retained pellet was lyophilized to a white powder. As shown in Figure 3A, the ¹³C CP-MAS spectrum of the pellet is dominated by the enriched carbonyl of [1-¹³C]Ala 4 at 171.4 ppm. When this sample is mixed with ~15 mL of the supernatant (Figure 1C) and lyophilized to a new white powder, both fibers and spherical oligomers are detected by TEM (Figure S7). The [1-¹³C] Ala4 carbonyl resonance however populates several distinct magnetic environments, resonating at 172.3 (6.5%), 172.9 (14.7%), 173.8 (6.3%), and 176 (6.6%) ppm, in addition to the fiber resonance at 171.4 ppm (Figure 3B).

These additional amide carbonyl resonance frequencies are all consistent with β -sheet secondary structure. The best resolved resonance at 176 ppm, which is slightly downfield of typical β -sheet backbone carbonyls, [15] is strongly dephased in $^{13}\text{C}(^{15}\text{N})$ REDOR analyses (Figure 3C, green) and fit to $64.6\pm8.6\%$

of the resonance arrayed as antiparallel β -sheets (Figure 3F). ¹³C-DQF-DRAWS also supports additional parallel β -sheet arrays resonating at the same chemical shift (Figure 3D, green). The multiplicity and broad line shape however limited accurate distance assignments (Figure S8),

The parallel in-register β-sheet strand arrangement expected for the peptide fiber at 171.4 ppm is confirmed in Figure 3D (red line). The ¹³C DQF-DRAWS analyses^[10,16] best fits to a repeating array of carbonyl carbons spaced 4.7 Å's apart as shown in Figure 3E. However, even the 171.4 ppm resonance shows greater dephasing in ¹³C{¹⁵N}REDOR analyses (Figure 3C, red) than seen for the pure fibers (Figure 3C black solid-line), indicating only $92.9 \pm 14\%$ of the enriched carbons exist in parallel β -sheets. With $^{13}\text{C}-^{15}\text{N}$ distances of 7.2 Å, 7.9 \pm 3.2% of the peptide would be assigned to anti-parallel β -sheets with distances to the adjacent stand ¹⁵Ns of 5.3 Å and 5.45 Å (Figure 3F). Even with these overlapping resonances, the T₂ for the 176 ppm resonance is 51.1 ± 2.0 ms, significantly less than the 171.4 ppm T_2 of 59.4 ± 1.4 ms (Figure S9), consistent with greater crystalline order existing within the parallel peptide fibers.[8f,g]

With this peptide congener, IR amide-I vibrational modes and NMR ^{13}C chemical shifts from isotopically enriched samples provide clear evidence for a mixture of β -sheet assemblies forming early in the liquid-like particle phase. Single β -sheets, maintained primarily by H-bonding in these dehydrated particle phases, are expected to be flexible, averaging the angular dependence of the exciton coupling that red shifts the electronic transitions underlying β -sheet assigned ellipticity. $^{[17]}$ Initial simulations suggest that such motions are expected to attenuate CD intensity more significantly than the H-bonding distances detected by IR and NMR spectroscopies.

Previous particle imaging experiments provide clear evidence for fiber nucleation occurring within metastable peptide particle phases. [8b,f, g] The diverse population of β -sheets documented here suggest, as with simulations of stable H-bonded chains of H_2O molecules existing in solution, [18] that H-bonding alone is sufficient to stabilize β -sheets in these peptide-rich phases. Product analyses have further suggested that facial complementarity of the β -sheet surfaces is critical for stable nucleation [8h,10,11d,19] and allows us to now propose the assembly pathway diagrammed in Figure 4. We propose that a critical threshold of β -sheets accumulate as the particle grows, and facial complementarity allows for selection of a stable nucleus that propagates in solution.

This detected population of single peptide β -sheets in two-step nucleation events^[19] could also respond to environmental templates, ranging from metals,^[12,13] nucleic acids,^[7] chemical reactions of the peptides,^[6a] as well as other peptide assemblies,^[6b,8b, f,g,10-11,20] each nucleating the growth of new assemblies. The generality of this model will now be further explored in the context of other intrinsically disordered protein domains^[21] and in full-length prions where the range of stable nuclei could be much greater.^[22]

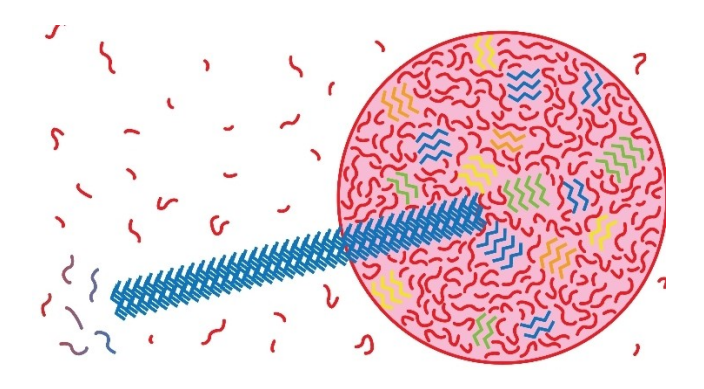


Figure 4. Proposed model for 2-step amyloid nucleation. Peptide strands (red lines) collapse into solute-rich particle phases. Within the particles, strands sample distinct β -sheets (orange, yellow, green, blue lines). Liquid-solid phase transition occurs through sheet lamination in the particle, propagating the selected structure (blue).

Experimental Section

Experimental details can be found in the Supporting Information.

Acknowledgements

We thank J. T. Goodwin for valuable discussions, the Robert P. Apkarian Microscopy Core for TEM access, and the Emory NMR Center for magnetic resonance access. The research was supported by grants from NSF CHE-1507932 for synthesis and NSF/DMR-BSF 1610377 for structural analysis, NIH Alzheimer's Disease Research Center: P50AG025688 for biological analyses, and Emory University for general support.

Conflict of Interest

The authors declare no conflict of interest.

Keywords: amyloid peptides · NMR spectroscopy · phase transitions · solid-state NMR · supramolecular assembly

- [1] a) A. F. Wallace, L. O. Hedges, A. Fernandez-Martinez, P. Raiteri, J. D. Gale, G. A. Waychunas, S. Whitelam, J. F. Banfield, J. J. De Yoreo, *Science* 2013, 341, 885–889; b) M. H. Nielsen, S. Aloni, J. J. De Yoreo, *Science* 2014, 345, 1158–1162.
- [2] Y. Shin, C. P. Brangwynne, *Science* **2017**, *357*.
- [3] T. Threlfall, Org. Process Res. Dev. 2003, 7, 1017-1027.
- [4] a) P. G. Vekilov, Soft Matter 2010, 6, 5254–5272; b) O. Annunziata, O. Ogun, G. B. Benedek, Proc. Mont. Acad. Sci. 2003, 100, 970–974; c) V. G. Taratuta, A. Holschbach, G. M. Thurston, D. Blankschtein, G. B. Benedek, J. Phys. Chem. 1990, 94, 2140–2144.
- [5] a) R. Tycko, Neuron 2015, 86, 632–645; b) A. W. P. Fitzpatrick, G. T. Debelouchina, M. J. Bayro, D. K. Clare, M. A. Caporini, V. S. Bajaj, C. P. Jaroniec, L. Wang, V. Ladizhansky, S. A. Müller, C. E. MacPhee, C. A. Waudby, H. R. Mott, A. De Simone, T. P. J. Knowles, H. R. Saibil, M. Vendruscolo, E. V. Orlova, R. G. Griffin, C. M. Dobson, Proc. Natl. Acad. Sci. USA 2013, 110, 5468–5473.
- [6] a) C. Chen, J. Tan, M. C. Hsieh, T. Pan, J. T. Goodwin, A. K. Mehta, M. A. Grover, D. G. Lynn, *Nat. Chem.* 2017, *9*, 799–804; b) J. E. Smith, C. Liang, M. Tseng, N. Li, S. Li, A. K. Mowles, A. K. Mehta, D. G. Lynn, *Isr. J. Chem.*



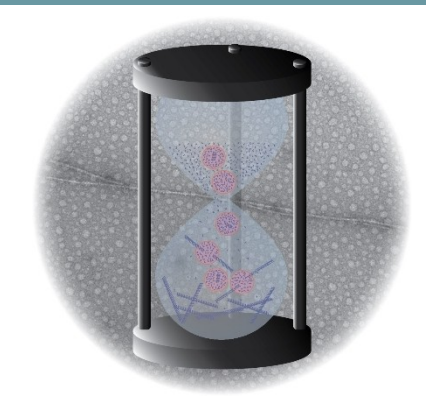
- **2015**, *55*, 763–769; c) J. Habchi, S. Chia, R. Limbocker, B. Mannini, M. Ahn, M. Perni, O. Hansson, P. Arosio, J. R. Kumita, P. K. Challa, S. I. A. Cohen, S. Linse, C. M. Dobson, T. P. J. Knowles, M. Vendruscolo, *Proc. Mont. Acad. Sci.* **2016**, *114*, 200–208.
- [7] A. Rha, D. Das, O. Taran, Y. Ke, A. Mehta, D. G. Lynn, Angew. Chem. Int. Ed. 2019.
- [8] a) V. J. Anderson, H. N. W. Lekkerkerker, *Nature* 2002, 416, 811–815;
 b) W. S. Childers, N. R. Anthony, A. K. Mehta, K. M. Berland, D. G. Lynn, *Langmuir* 2012, 28, 6386–6395;
 c) S. Arya, A. K. Singh, T. Khan, M. Bhattacharya, A. Datta, S. Mukhopadhyay, *J. Phys. Chem. Lett.* 2016, 7, 4105–4110;
 d) M. C. Hsieh, C. Liang, A. K. Mehta, D. G. Lynn, M. A. Grover, *J. Am. Chem. Soc.* 2017, 139, 17007–17010;
 e) M. G. Iadanza, M. P. Jackson, E. W. Hewitt, N. A. Ranson, S. E. Radford, *Nat. Rev. Mol. Cell Biol.* 2018, 19, 755–773;
 f) N. R. Anthony, K. M. Berland, A. K. Mehta, D. G. Lynn, W. Seth Childers, in *Bio-nanoimaging* (Eds.: V. N. Uversky, Y. L. Lyubchenko), Academic Press, Boston, 2014, pp. 27–36;
 g) N. R. Anthony, A. K. Mehta, D. G. Lynn, K. M. Berland, *Soft Matter* 2014, 10, 4162–4172;
 h) A. K. Mehta, K. Lu, W. S. Childers, Y. Liang, S. N. Dublin, J. Dong, J. P. Snyder, S. V. Pingali, P. Thiyagarajan, D. G. Lynn, *J. Am. Chem. Soc.* 2008, 130, 9829–9835.
- [9] a) E. Karran, M. Mercken, B. D. Strooper, *Nat. Rev. Drug Discovery* 2011, 10, 698–712; b) D. M. Holtzman, J. C. Morris, A. M. Goate, *Sci. Transl. Med.* 2011, 3, 77sr71.
- [10] C. Liang, R. Ni, J. E. Smith, W. S. Childers, A. K. Mehta, D. G. Lynn, J. Am. Chem. Soc. 2014, 136, 15146–15149.
- [11] a) C. Hilbich, B. Kisters-Woike, J. Reed, C. L. Masters, K. Beyreuther, J. Mol. Biol. 1992, 228, 460–473; b) S. J. Wood, R. Wetzel, J. D. Martin, M. R. Hurle, Biochemistry 1995, 34, 724–730; c) L. O. Tjernberg, J. Naslund, F. Lindqvist, J. Johansson, A. R. Karlstrom, J. Thyberg, L. Terenius, C. Nordstedt, J. Biol. Chem. 1996, 271, 8545–8548; d) J. Dong, J. M. Canfield, A. K. Mehta, J. E. Shokes, B. Tian, W. S. Childers, J. A. Simmons, Z. Mao, R. A. Scott, K. Warncke, D. G. Lynn, Proc. Natl. Acad. Sci. USA 2007, 104, 13313–13318.
- [12] J. Dong, R. P. Apkarian, D. G. Lynn, Bioorg. Med. Chem. 2005, 13, 5213– 5217.

- [13] a) D. M. Morgan, J. Dong, J. Jacob, K. Lu, R. P. Apkarian, P. Thiyagarajan, D. G. Lynn, J. Am. Chem. Soc. 2002, 124, 12644–12645; b) C. Yuan, A. Levin, W. Chen, R. Xing, Q. Zou, T. W. Herling, P. K. Challa, T. P. J. Knowles, X. Yan, Angew. Chem. Int. Ed. 2019, 58, 18116–18123.
- [14] J. W. Brauner, C. Dugan, R. Mendelsohn, J. Am. Chem. Soc. 2000, 122, 677–683.
- [15] D. S. Wishart, B. D. Sykes, F. M. Richards, *J. Mol. Biol.* **1991**, *222*, 311–333.
- [16] a) T. L. S. Benzinger, D. M. Gregory, T. S. Burkoth, H. Miller-Auer, D. G. Lynn, R. E. Botto, S. C. Meredith, *Proc. Mont. Acad. Sci.* 1998, 95, 13407–13412; b) P. Liu, R. Ni, A. K. Mehta, W. S. Childers, A. Lakdawala, S. V. Pingali, P. Thiyagarajan, D. G. Lynn, *J. Am. Chem. Soc.* 2008, 130, 16867–16869; c) J. R. Long, J. L. Dindot, H. Zebroski, S. Kiihne, R. H. Clark, A. A. Campbell, P. S. Stayton, G. P. Drobny, *Proc. Natl. Acad. Sci. USA* 1998, 95, 12083–12087; d) M. A. Mehta, M. T. Eddy, S. A. McNeill, F. D. Mills, J. R. Long, *J. Am. Chem. Soc.* 2008, 130, 2202–2212.
- [17] a) N. Sreerama, R. Woody, Circular Dichroism of Peptides and Proteins, John Wiley and Sons, New York, 2000; b) M. Abdellatief, M. Abele, M. Leoni, P. Scardi, J. Appl. Crystallogr. 2013, 46, 1049–1057; c) F. Formaggio, C. Peggion, M. Crisma, B. Kaptein, Q. B. Broxterman, J. P. Mazaleyrat, M. Wakselman, C. Toniolo, Chirality 2004, 16, 388–397.
- [18] S. Naserifar, W. A. Goddard, Proc. Mont. Acad. Sci. 2019, 116, 1998–2003.
- [19] M. A. Vorontsova, D. Maes, P. G. Vekilov, Faraday Discuss. 2015, 179, 27– 40
- [20] M. C. Hsieh, D. G. Lynn, M. A. Grover, J. Phys. Chem. B 2017, 121, 7401–7411
- [21] K. J. Niklas, A. K. Dunker, I. Yruela, J. Exp. Bot. 2018, 69, 1437-1446.
- [22] M. Ziaunys, T. Sneideris, V. Smirnovas, Sci. Rep. 2020, 10, 4572-4578.

Manuscript received: January 20, 2020 Accepted manuscript online: April 10, 2020 Version of record online:

COMMUNICATIONS

Sheet complementarity directs assembly: Amyloid disease progression begins with neurotoxic oligomeric particles that transition into paracrystalline peptide fibrils. Here we show with a model amyloid peptide that oligomer particles contain multiple β -sheet assemblies prior to nucleation where sheetsheet lamination dictates the structure of the emerging fibril.



Dr. R. F. Rengifo, A. Sementilli, Y. Kim, Dr. C. Liang, Dr. N. X.'A. Li, Dr. A. K. Mehta*, Dr. D. G. Lynn*

1 - 5

Liquid-Like Phases Preorder Peptides for Supramolecular Assembly

